Journal of Theoretical and Applied Information Technology
30th November 2012. Vol. 45 No.2

ISSN: 1992-8645 www.jatit.org E-ISSN: 1817-3195

AERODYNAMIC ANALYSIS AND WIND TUNNEL TEST FOR FLAPPING-WING MAVS

[1] LAN LIU, [1]XIJING ZHANG, [2]ZHAOXIA HE
[1] School of Mechanical Engineering, Northwestern Polytechnical University, Xi'an 710072, China
[2] Key Laboratory of Road Construction Technology and Equipment, Ministry of Education, Chang'an University, Xi'an 710064, China

ABSTRACT

A lightweight flapping-wing micro air vehicle (MAV) was designed and built and successfully filed in the sky. The unsteady aerodynamics associated with this MAV was detailedly studied by using the method of computational fluid dynamics (CFD).The variations of different parameters of the flapping MAV, such as flapping amplitude, pitch amplitude and flapping frequency, were investigated with numerical simulation. The Fluid-Structure coupling mechanics for flexible flapping-wings were subsequently researched and discussed. According to the practically developed MAV, a 2-D model for flexible flapping-wings was established. Fluid-Solid interaction deformation and its effects on the aero dynamic performance were analyzed, which offers a theoretical basis for design of the aircraft with flexible flapping-wing. The results of numerical simulation for the rigid and flexible flapping-wings were finally verified by conduct the aerodynamic performance tests in a low turbulence and low Reynolds number wind tunnel.

Keywords: *Flapping-wing MAV, Flexible Wings, Fluid-Solid Interaction, Wind Tunnel Test*

1 INTRODUCTION

Flapping-wing micro air vehicle (Flapping-wing MAV) is a new conceptual aircraft which mimics the flying modes of birds and insects and can be widely used in various fields of military and civil applications. Flapping-wing MAVs are usually of small sizes and light weights, with low manufacturing costs, good stealth abilities and high maneuverability. Considering its characteristics and advantages, flapping-wing MAVs have a broad and promising prospect and will be widely researched in the near future.

From the end of 1980's, many experimental researches which focused on rigid airfoils [1-3] were carried out to investigate the effects of oscillation mode [4-6], and aspect ratio[7]. The special case of hovering flight also received researchers' attention [8-9]. However, the effects of wing stiffness, either in the chordwise or spanwise direction, were relatively unexplored by the researchers. This is surprising considering the importance of flexibility to fishlike wings [10], and the finding of intricate variations in the stiffness of insect wings[11], though the role of flexibility for insect wings is still unclear [12]. The effect of chordwise flexibility on an airfoil in heave at low Reynolds numbers has been studied by Heathcote and Gursul [13]. Particle Image Velocimetry measurements revealed a correspondingly stronger jet vortex pattern. And chordwise flexibility is also found to be able to bear efficiency benefits [14].

The most outstanding characteristic of the wings of the small flying insects is its elaboration and softness. This enables the insects to distort their wings to change the attack angle efficiently during flying. However, the current Integrated Circuit(IC) fabrication technology, with which we used to make a wing model, is still not capable of making such flexible and complicated parts easily. The purpose of this research on biomimetic wings is not to imitate absolutely insect's wings but to summarize some common characteristics by computation and observation to design a typical biomimetic wing.

2 THE AERODYNAMIC MODEL AND ANALYSIS OF RIGID WINGS

2.1 Flapping-Wing Model

Figure 1 shows a flapping-wing MAV designed and manufactured by our research group. It could imitate the flapping motions of small birds and insects along two directions - flapping and pitching.

In Figure2, The airframe along Z direction and the trailing-edge of wings fixed on the body define

Journal of Theoretical and Applied Information Technology
30th November 2012. Vol. 45 No.2

ISSN: 1992-8645 www.jatit.org E-ISSN: 1817-3195

obliquity angel β between wings plane and airframe. The wing's leading-edge flaps as an actuator and α is defined as the flapping angle in wing's leading-edge plane (XOY). Due to the trailing-edge of wings fixed on the body, β also changes in plane YOZ as wings leading-edge flap and it makes wings produce pitching motion.

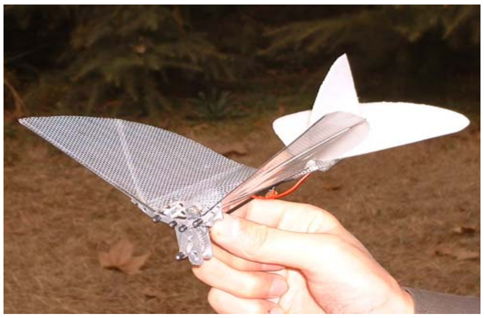

Figure 1: Battery-Powered Flapping-Wing MAV

The flapping angel and pitching angle could be given by:

$$\alpha(t)=\alpha_0+\frac{A_0}{2}(\cos\omega t) \tag{1}$$

$$\beta(t)=\beta_0+\frac{B_0}{2}(\cos\omega t) \tag{2}$$

in which ω is flapping frequency, A_0 is flapping amplitude, α_0 is initial flapping angle, B_0 is pitching amplitude, and β_0 is initial incline angle.

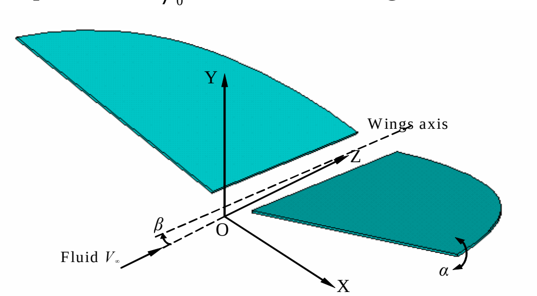

Figure 2: Sketches Of The Reference Frames And Wing Motion

2.2 N-S Equations And Compute Methods

In coordinates system XOYZ, the N-S equations can be obtained in non-dimension form:

$$\frac{\partial u}{\partial X}+\frac{\partial v}{\partial Y}+\frac{\partial w}{\partial Z}=0 \tag{3}$$

$$\frac{\partial u}{\partial \tau}+u\frac{\partial u}{\partial X}+v\frac{\partial u}{\partial Y}+w\frac{\partial u}{\partial Z}=-\frac{\partial P}{\partial X}+\frac{1}{\mathrm{Re}}\left(\frac{\partial^2 u}{\partial X^2}+\frac{\partial^2 u}{\partial Y^2}+\frac{\partial^2 u}{\partial Z^2}\right) \tag{4}$$

$$\frac{\partial v}{\partial \tau}+u\frac{\partial v}{\partial X}+v\frac{\partial v}{\partial Y}+w\frac{\partial v}{\partial Z}=-\frac{\partial P}{\partial Y}+\frac{1}{\mathrm{Re}}\left(\frac{\partial^2 v}{\partial X^2}+\frac{\partial^2 v}{\partial Y^2}+\frac{\partial^2 v}{\partial Z^2}\right) \tag{5}$$

$$\frac{\partial w}{\partial \tau}+u\frac{\partial w}{\partial X}+v\frac{\partial w}{\partial Y}+w\frac{\partial w}{\partial Z}=-\frac{\partial P}{\partial Z}+\frac{1}{\mathrm{Re}}\left(\frac{\partial^2 w}{\partial X^2}+\frac{\partial^2 w}{\partial Y^2}+\frac{\partial^2 w}{\partial Z^2}\right) \tag{6}$$

where u , v and w are the non-dimension velocity in the direction of X, Y and Z. P is non-dimension pressure. For the analysis of non-dimension, the reference velocity, the length and the time are assigned as U, c and c/U respectively, while U is the average velocity when wings flapping in fully cycle.

Reynolds number defines as:

$$\mathrm{Re}=cU/\nu \tag{7}$$

ν is the motion viscosity number.

At the beginning, supposing the flapping-wing MAV is static and starts flying at t=0, so the flow field should satisfy the initial condition:

$$\vec{V}_{t=0}=\vec{V}_\infty=u_\infty\vec{i}+v_\infty\vec{j}+w_\infty\vec{k} \tag{8}$$

where $\vec{V}_\infty$ is the velocity at the indefinitely faraway place. When flapping-wing MAV is hovering or suspending, $\vec{V}_\infty$ equals to zero; when it flies forward, the velocity will change to its opposite direction. $\vec{i}$ 、 $\vec{j}$ 、 $\vec{k}$ are the directional unit vector in Plane OXYZ.

On the surface of wings, the flow field should meet the condition of non-slip surface:

$$\vec{V}_C=\vec{V}_{wing} \tag{9}$$

C is the boundary curve surface, $\vec{V}_{wing}$ is the instantaneous velocity of boundary points. At the indefinitely faraway, flow field condition is:

$$\vec{V}_{(x,y,z)\to\infty}=\vec{V}_\infty \tag{10}$$

Equations (3)~(10) are the motion equations of fluid in the inertial coordinates. In general, the problem can be resolved by solving these equations. But it is difficult to carry out related numerical computation considering the wings's boundary is constantly changing as MAV flaps. In order to solve the large scale moving boundary problem, Arbitrary Lagrangian Eulerian (ALE) finite element method in ANSYS/CFD is adopted. After solving the N-S equations, the velocity and pressure of each node in every time step can be derived from the fluid field. The aerodynamic forces, which are composed of pressure and cut force, integrated wings surface pressure and viscosity force, can be obtained at that time. The lift force L and drag force along Y and Z direction can also be obtained. And lift coefficient and drag coefficient can be calculated by:

Journal of Theoretical and Applied Information Technology
30th November 2012. Vol. 45 No.2

ISSN: 1992-8645 www.jatit.org E-ISSN: 1817-3195

$$C_L = \frac{L}{0.5\rho_{air}U^2S} \tag{11}$$

$$C_D = \frac{D}{0.5\rho_{air}U^2S} \tag{12}$$

And ρ_{air} is the air density; S is characteristic area.

2.3 Results and Analysis

To validate the method, the calculated lift and drag coefficients with NACA rectangle wings are compared with the experiment results. The air density for calculation is $\rho_{air} = 1.225\times10^{-3} g/cm^3$; the viscosity coefficient is $\nu = 1.0 cm^2/s$, and the attack angle varies from 0 degree to 90 degree. The calculated results are shown as Figure 3(a). And Figure 3(b) shows the experiment results from Dickson[15].

In Figure 3, the horizontal axis denotes the magnitude of attack angle; the vertical axis denotes the magnitude of lift and drag coefficients. It shows that the lift and drag coefficients calculated by the numerical method resemble the experiment results, though they are a bit lower than the experiment results. This distinction may origins from the difference of geometry between computing model and experiment model.

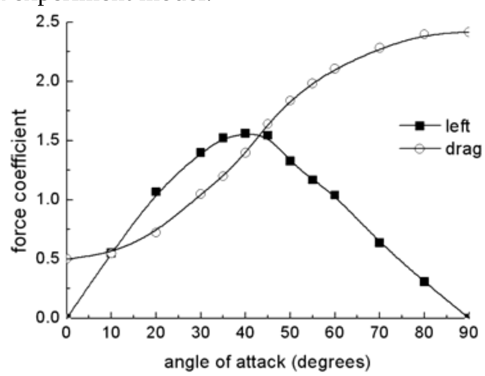

(A) Proposed Calculated Results

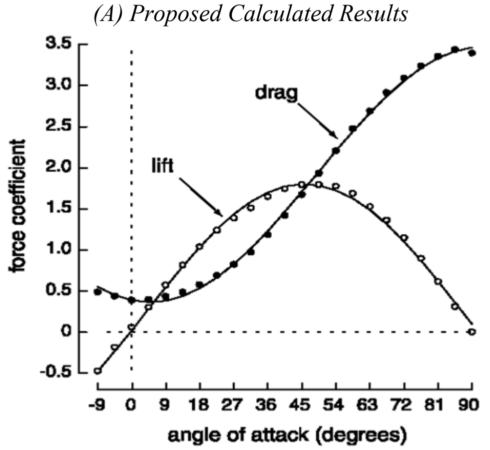

(B) Dickinson's Experimental Results

Figure 3: Wing Lift And Wing Drag Per Unit Span Versus Time Of Insect Hovering Flight

2.4 Forward Flight Of Flapping-Wing MAV

2.4.1 Calculation of Lift and Drag force

Parameters based on the manufacturing Flapping-wing MAV are as follow: wings span is 200mm; chord length is 70mm; each wing's shape is a quarter of ellipse and its area is 100 cm^2; flapping frequency f = 10Hz; flapping amplitude $A_0 = \pi/3$; initial flapping angle $\alpha_0 = \pi/12$; initial pitching angle $\beta_0 = \pi/18$; air density $\rho_{air} = 1.225\times10^{-3} g/cm^3$; viscosity $\nu = 1.0 cm^2/s$; forward flight velocity $\vec{V}_\infty = 5m/s$; Reynolds number 2500. When numerical solution is approaching to stability, the lift and drag force varied with time can be shown in Figure 4.

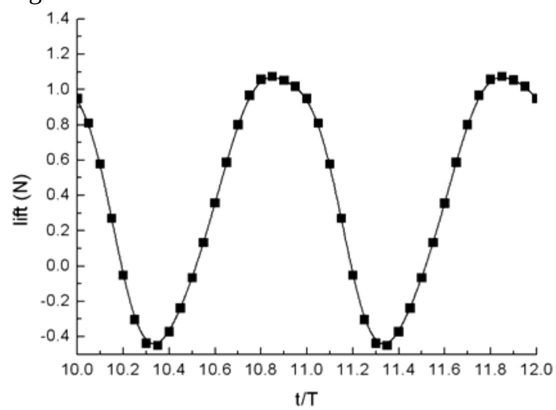

(A) Lift-Time Curve

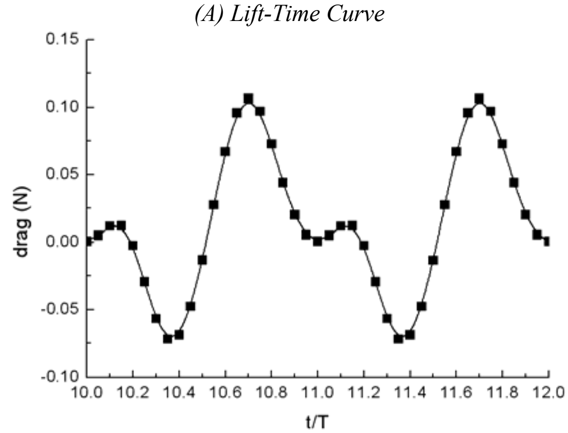

(B) Drag-Time Curve

Figure 4: Wing Lift And Wing Drag Per Unit Span Versus Time Of MAV Flapping Flight

In Figure 4 the horizontal axis denotes non-dimension time t/T(which T is the period); vertical axis is lift and drag force per span and its unit is Newton. In a whole cycle, the instantaneous max value L_{max} is 1.07N and the average lift $\overline{L}$ =

Journal of Theoretical and Applied Information Technology
30th November 2012. Vol. 45 No.2

ISSN: 1992-8645 www.jatit.org E-ISSN: 1817-3195

0.38N in each wing span. The weight of flapping-wing MAV is 15g, and the corresponding flapping lift of instantaneous value is 109.2g which is 7 times to its weight. The average lift is 38.7g which is 2.5 times to its weight. Obviously, the lift produced by flapping can overcome it self-weight to fly freely.

2.4.2 Flapping Parameter to Flight

In fabricating flapping-wing MAV, some parameters have great influence on its flight ability. In the paper, two major parameters, flapping frequency and flapping amplitude, are taken to calculate the lift and drag coefficients. and their corresponding results are compared to each other. Figure 5 and Figure 6 show the average lift and drag coefficient curve changing/varying with flapping amplitude (20~90 degree) when others parameter are kept unchanged; While Figure 7 and Figure 8 show that changing the flapping frequency (2~15Hz), and get lift and drag coefficient curve.

From Figure 5 to 8, we can see that the flapping frequency and the flapping amplitude have direct influence on lift force. The bigger the flapping amplitude or the flapping frequency, the bigger the lift force. Besides, lift is sensitive to frequency when the flapping frequency is of a small value. As frequency increases to some value, the non-dimension average lift force approaches to stability.

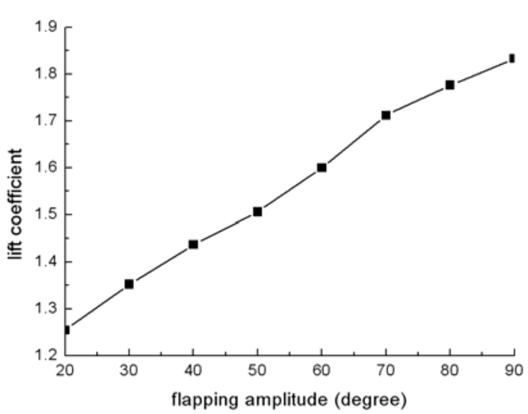

Figure 5: Lift Coefficient Versus Different Flapping Amplitude

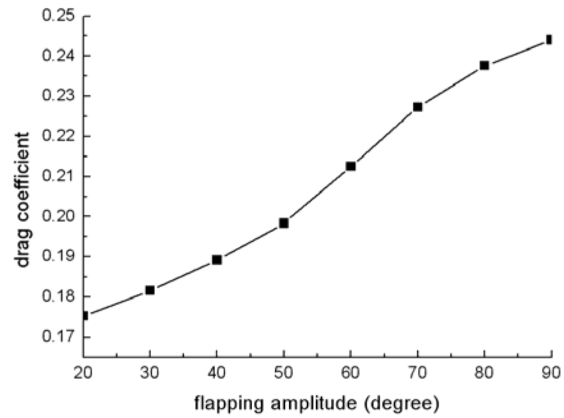

Figure 6: Drag Coefficient Versus Different Flapping Amplitude

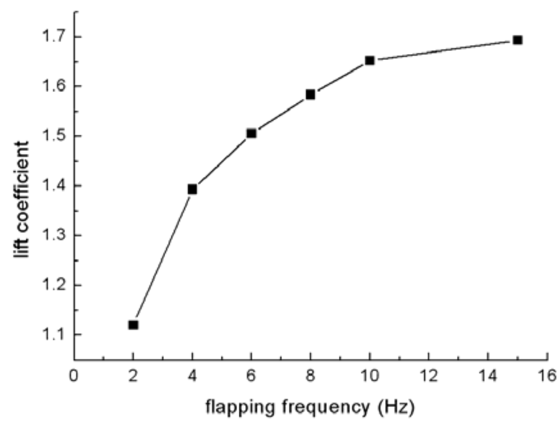

Figure 7: Lift Coefficient Versus Different Flapping Frequency

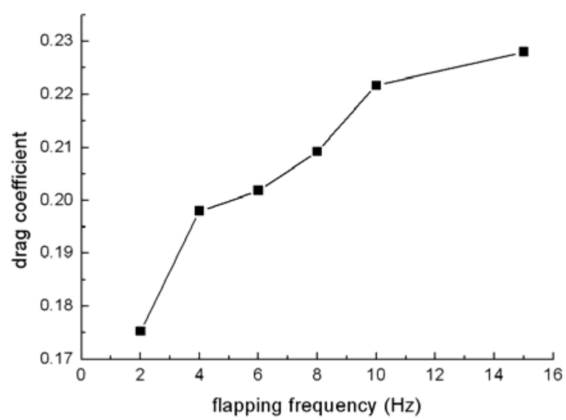

Figure 8: Drag Coefficient Versus Different Flapping Frequency

3 THE AERODYNAMIC MODEL AND ANALYSIS OF RIGID WINGS

In our design, the leading-edge is rigid but the trailing-edge is flexible. So, the flexible deformation is mainly in the chord direction. It can be simplified

Journal of Theoretical and Applied Information Technology
30th November 2012. Vol. 45 No.2

ISSN: 1992-8645 www.jatit.org E-ISSN: 1817-3195

as a two-dimension flexible model in the chord section.

3.1 Flapping Model In Two Dimension

Figure 9 shows the flapping motion model in two dimension. The horizontal axis is along the centre line of MAV's body. The leading-edge is rigid and can flapp up and down around vertical axis. The trailing-edge is flexible and is fixed on point A by using moveable equipment in chord direction which can make it pitch as flapping. Supposing the pitching amplitude B_0 and β_0 is assemble angle defined by wings and body; point A has coordinate (x_A, y_A) and flapping frequency is f and flapping signal is sin wave, the motion relation can be expressed in any point of wings as:

$$y = (x_A - x)\sin[B_0 \sin(2\pi ft + \beta_0)] \quad (13)$$

In flapping model, chord C=50mm and thick h=0.5mm; material properties such as elastic module E=100GPa, $\rho = 1200\text{kg/m}^3$, $\mu = 0.25$, forward flight velocity $V_\infty = 5\text{m/s}$, pitching amplitude $B_0 = 15°$, assemble angle $\beta_0 = 6°$, flapping frequency f=10Hz.

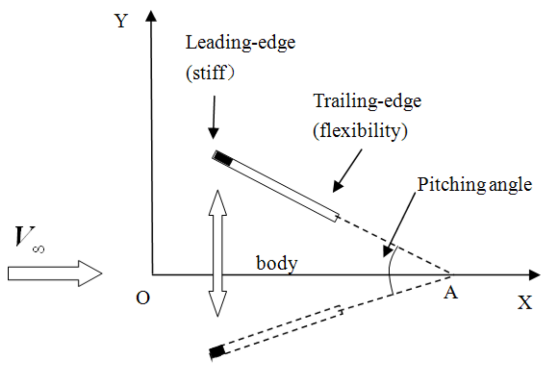

Figure 9: Flapping Model With Two Dimension

3.2 Fluid-Solid interaction Deformation Results

When coupling iterative calculation is over and convergent, the deformation results with flapping aerodynamic can be obtained as shown in Figure 10.

Figure 10(a) is the deformation results in downstroke, and (b) is the deformation results in upstroke. We can see that wings have obviously deformed, especially in trailing-edge. The calculation result shows the max deformation is about 1/10 of chord length. Changing model's stiffness and increasing model's flexibility, the deformation amount can be larger. In addition, deformation direction is opposite to flapping direction. Due to air drag force and inertia force, deformation and flapping do not synchronize with each other but in the different phases. Figure 11 shows deformation occurs in the instantaneous between downstroke and upstroke when motion is going to be stable.

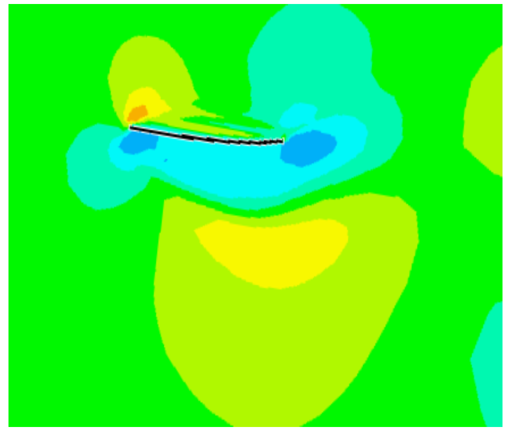

(a) Downstroke

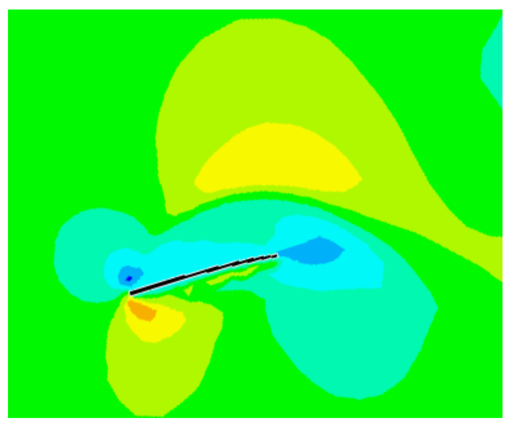

(b) Upstroke

Figure 10: Deformation By Aerodynamic

Figure 11(a) occurs in the position where the wing has completed the upstroke and started the downstroke. There is a leading-edge vortex in leading-edge which suggests that leading-edge start the downstroke while trailing-edge still in its upstroke. Figure 11(b) just shows in relative position where the wings has completed the downstroke and started its upstroke. The difference in phase may lead to quickly torsion in trailing-edge of flexible wings when it switches from upstroke to downstroke. It just is similar to the insects' wings motion. Although its amplitude is small, this motion has produce sufficient lift force and drag force in some way.

Journal of Theoretical and Applied Information Technology
30th November 2012. Vol. 45 No.2

ISSN: 1992-8645 www.jatit.org E-ISSN: 1817-3195

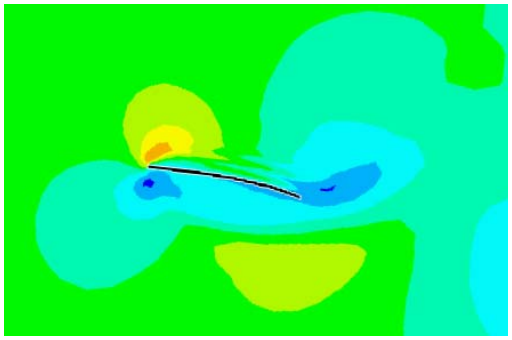

(a) Start Downstroke

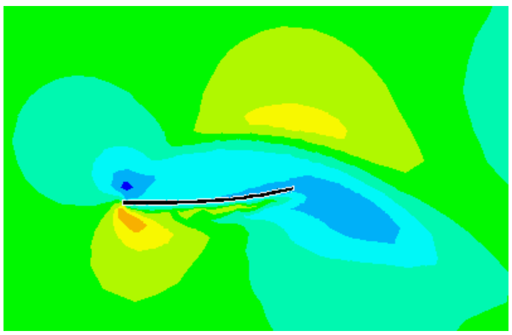

(b) Start Upstroke

Figure 11: Instantaneous Deformation During Flapping

3.3 Aerodynamic Character Of Flexible Wings Model

The influences of flexible wings are studied by comparing lift force and drag force produced by rigid wings and flexible wings. Flapping model is shown as Figure 9. The lift force and drag force of rigid wings and flexible wings can be calculated respectively. In Figure 12, vertical coordinate defines the ift force and drag lift in per wings span. Negative lift force is quite near between rigid wings and flexible wings. When the positive lift increases, the average lift force also increases (from 72.6g/m to 91.2g/m). The wings span is 200mm and the total lift force is 3.73g. It can be explained by torsion effect which suddenly changes direction in upstroke and downstroke. It also can be seen from the peak and valley of the lift curve wave.that if the drag force changes greatly in flexible wings, the average drag lift from 4.29g to 11.42g which is 7 times compared with that produced by the rigid wings. It can be explained that deformation opposite to flapping direction during the upstroke and downstroke will lead to increased force in horizontal direction.

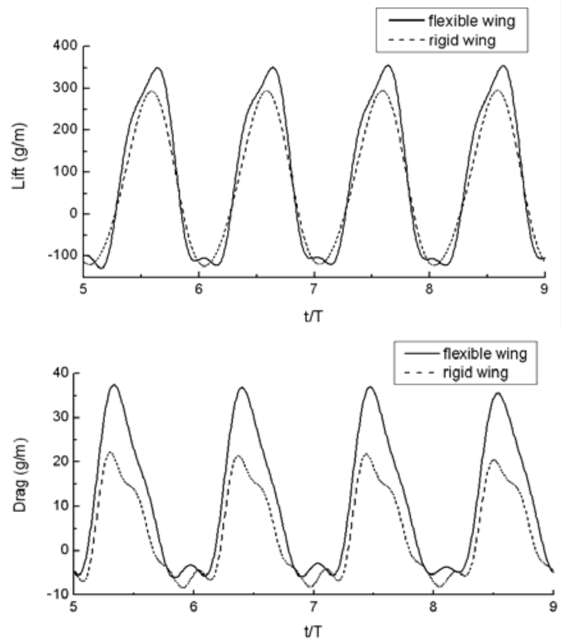

Figure 12: Lift And Drag Force Produced By Rigid Wings And Flexible Wings

Obviously, the flexible wings play an important role in producing drag lift while the rigid wings can't or only produce little drag lift. So, it is important to make wings flexible when designing a flapping-wing MAV. As the function of flexible deformation of trailing-edge is similar to that of a fan propel air flow in backward, the drag lift make flapping-wing MAV fly forwardly.

4 EXPERIMENT

It is expected that the flexible wings will affect the lift force. In order to study the effect of the wing flexibility on the lift force of a flapping wing, two different wings were constructed for the wind tunnel test of the lift force. The two kinds of wings are of span of 300mm and with aspect ratio 2 and are referred as type A and B respectively as shown in Figure 13. Type A is the rigid wings which are constructed by epoxy reinforced light wood and covered with a PVC plastic film. Type B is the flexible wings which are constructed by carbon fiber composite frames. The weight of the whole flapping wing MAV is 16g.

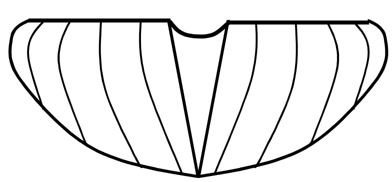

(a) Type A: Rigid Wing

Journal of Theoretical and Applied Information Technology
30th November 2012. Vol. 45 No.2

ISSN: 1992-8645 www.jatit.org E-ISSN: 1817-3195

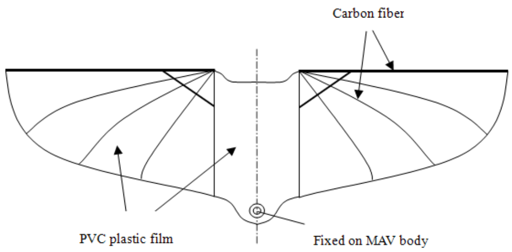

(b) Type B: Flexible Wing

(c) The Model Of Flapping Wing MAV

Figure 13: Different Wing Constructions And The Model Of Flapping Wing MAV

During the wind tunnel test of the flapping wings, four different attack angles, 0, 10, 20 and 30 degrees, were used. The angle of attack is formed by attached the wing to the driving unit with a specific angle. The angle of attack is defined according to the wind-axes reference frame. The different wind velocities used for the test are 0 to 5m/sec in a step increase of 1m/sec. Load cells were mounted on the base of the driving unit to measure the lift force or thrust on the wind tunnel test. The capacity of the load cell is 200g with an excitation voltage of 5V. Standard weights were used to calibrate the load cell before our tests. The signal from the load cell was recorded directly by a measurement system, CRAS-AZ216R. The recording duration is 4 seconds with 2500 digital points that can be downloaded to a personal computer after the test. Before a test, the initial weight of the entire assembly above the load cell was recorded. As the wings start to flap, the oscilloscope will record the load variation during the preset duration. The lift during the flapping motion can be derived by subtracting the measured load from the initial weight. The average lift can be calculated by average the lift along the measured time span. The lift and thrust were measured with respect to the wind-axes reference frame. The setups of the flapping wings for lift wind tunnel tests are shown in Figure 14.

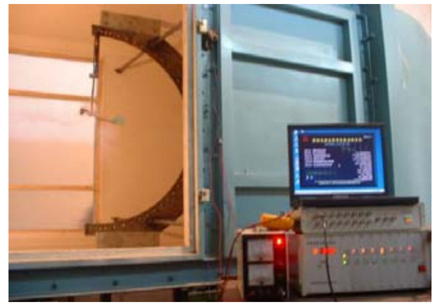

Figure 14 Measurement System Of Wind Tunnel

In order to study the different effects of the rigid wing and flexible wing on the lift force, we tested the average lift forces of the two types of wings under the same flapping frequency (4Hz) and wind speeds (0m/s and 4m/s) for different angles of attack, as shown in Figure 15 and Figure 16.

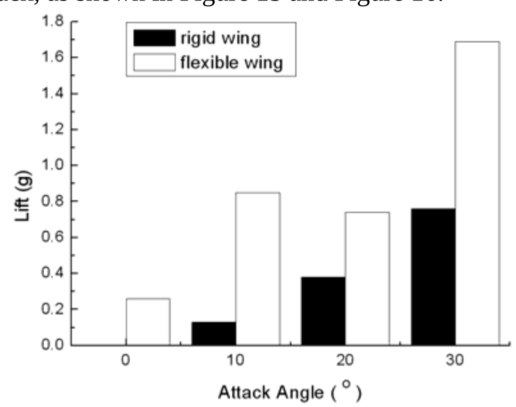

Figure 15: Average Lift Versus Attack Angle When Wind Velocity Is 0m/S

It is shown that the lift force of flexible wing is higher than that of rigid wing in any case. Due to the flexibility of type B wing, the second mode deformation is induced for a higher flapping frequency. Under this situation of second mode deformation, the lift force is saturated or even decreases.

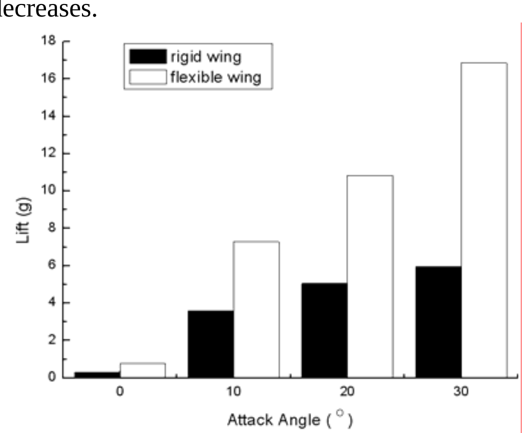

Figure 16: Average Lift Versus Attack Angle When Wind Velocity Is 4m/S

Journal of Theoretical and Applied Information Technology
30th November 2012. Vol. 45 No.2

ISSN: 1992-8645 www.jatit.org E-ISSN: 1817-3195

It is shown that the lift force of flexible wing is higher than that of rigid wing in any case. Due to the flexibility of type B wing, the second mode deformation is induced for a higher flapping frequency. Under this situation of second mode deformation, the lift force is saturated or even decreases.

The lift forces for different flapping frequencies and wind speeds are shown in Figure 17 by using the flexible wing type B. Figure 17 also gives the lift forces for different angles of attack. It is shown that there is no lift force without the relative wind speed. Although the flapping angles are different in upstroke and downstroke, the upward force and the downward force are roughly the same during the entire flapping cycle and tend to counteract each other in this situation. Increase of the flapping frequency will also induce lift force. With a relative wind speed, a lift force can be generated and higher lift force is induced if a higher angle of attack. It is demonstrated that the relative wind speed and the angle of attack are the major factors for the lift force of an ornithopter under a simple flapping motion.

The lift force increases substantially at the high wind speed. That means flying at higher speed is more effective a way in obtaining the required lift force rather than increasing the flapping frequency. In the experimental wind tunnel tests, the wind speed and flapping frequency are kept as separated independent variables. However, in the actual flight, the flying speed that can be reached depends on the flapping frequency of the wings. In order to increase the flying speed, the flapping frequency must be increased accordingly.

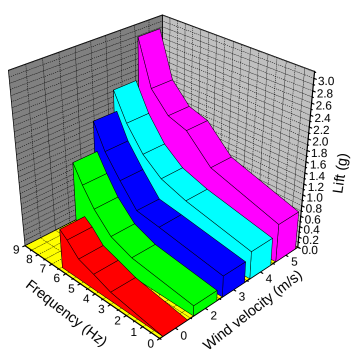

(A) Attack Angle Is 0 Degree

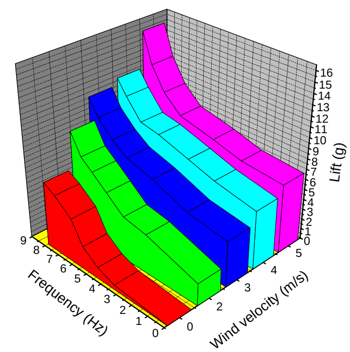

(B) Attack Angle Is 10 Degree

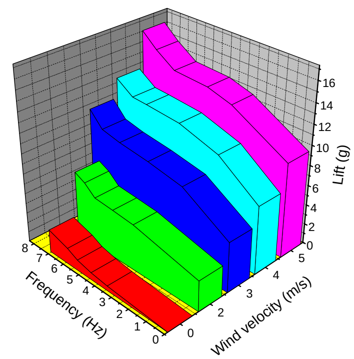

(C) Attack Angle Is 20 Degree

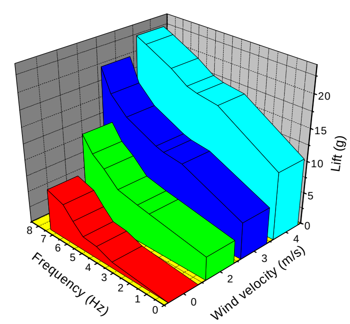

(D). Attack Angle Is 30 Degree

Figure 17: Average Lift Versus Frequency And Wind Velocity When Attack Angle Is Vary

5 CONCLUSION

A three dimensional movable wing model was built for the flapping MAV, which mimics biological locomotion. The Arbitrary Lagrangian Eulerian (ALE) method with ANSYS/CFD was used to solve the Navier-Stokes equations numerically. The solution supposes that the leading-edge vortices could generate enough lift to support a typical flapping MAV. With numerical simulation, the variations of different parameters of the flapping

ISSN: 1992-8645 www.jatit.org E-ISSN: 1817-3195

MAV, such as flapping amplitude, pitch amplitude and flapping frequency, were studied.

The Fluid-Solid interaction mechanics for flexible flapping-wing had been preliminarily studied and discussed. According to the practically developed MAV, a two-dimensional model for flexible flapping-wing had been established. Fluid-Solid interaction deformation and the effects of this model on the aero dynamic performance were analyzed, which offers a theoretical basis for design of the aerocraft with flexible flapping-wing.

Based on the assumption of geometric similarity among birds and insects, the bionic design method for rigid and flexible flapping-wings was studied and a lightweight flapping-wing MAV was build which can successful fly in the sky. Then aerodynamic performance tests have been conducted for the manufactured rigid and flexible flapping-wings in a low turbulence and low Reynolds number wind tunnel at NPU (Northwestern Polytechnical University). The test results proved that the lift performance of flexible wing is better than rigid wing. The influences of flapping frequency, wind velocity and angle of attack on aerodynamic characteristics were investigated. During the wind tunnel test, the composite parts of flapping lift and their relations between each other were discussed. The test was successful and the results could be helpful for the design of flapping-wing MAV.

ACKNOWLEDGEMENTS

This work was supported by National Natural Science Foundation of China (51175426), Natural Science Basic Research Plan in Shaanxi Province of China(2012JM7010)and the Special Fund for Basic Scientific Research of Central Colleges, Chang'an University (CHD2011JC177).

REFRENCES:

[1] Koochesfahani, M.M., "Vortical patterns in the wake of an oscillating airfoil", AIAA Journal, No.27, 1989, pp. 1200-1205.

[2] Jones, K. D., Dohring, C.M., Platzer, M.F., "Experimental and computational investigation of the Knoller-Betz effect", AIAA Journal, No.36, 1998, pp. 1240-1246.

[3] Lai, J.C., Platzer, M.M., "Jet characteristics of a plunging airfoil", AIAA Journal, No.27, 1999, pp. 1200-1205.

[4] EMblemsvag, J. E., Suzuki, R., Candler, G. V., "Simulation of a three-dimensional flapping cantilever for micro air vehicle propulsion", 33rd AIAA Fluid Dynamics Conference (2003), AIAA Paper 2003-4012,

[5] Anderson, J.M., Streitlien, K., Barrett, D.S., Triantafyllou, M.S., "Oscillating foils of hight propulsive efficiency", Journal of Fluid Mechanics, No.360, 1998, pp. 41-72.

[6] Hover, F.S., Haugsdal, O., Triantafyllou, M.S., "Effect of angle of attact profiles in flapping foil propulsion", Journal of Fluids and Structures, No.19, 2004, pp. 37-47.

[7] Jones, K.D., Castro, B.M., Mahmoud, O., Pollard, S.J., Platzer, M.F., Gonet, K., Hummel, D., "A collaborative numberical and experimental investigation of flapping-wing propulsion", 40th Aerospace Sciences Meeting &Exhibit (2002), AIAA Paper 2002-0706.

[8] Freymuth, P., "Thrust generation by an airfoil in hover modes", Experiments in Fluids, No. 9, 1990, pp.17-24.

[9] Sunada, S., Kawachi, K., Matsumoto, A., Sakaguchi, A., "Unsteady force on a two-dimensional wing in plunging and pitching motions", AIAA Journal, No.39, 2001, pp.1230-1239.

[10] Triantafyllou, M.S., Triantafyllou, G.S., Yue, D.K.P., "Hydrodynamic of fishlike swingming", Annual Review of Fluid Mechanics, No. 32, 2000, pp.33-53.

[11] Wootton, R.J., "Support and deformability in insect wings", Journal of Zoology London, No.193, 1981, pp. 447-468.

[12] Maxworthy, T., "The fluid dynamics of insect flight", Annual Review of Fluid Mechanics, No.13, 1981, pp. 329-350.

[13] Healthcote, S., Gursul, I., "Flexible flapping airfoil propulsion at low Reynolds numbers", 43rd AIAA Aerospace Sciences Conference and Exhibit(2005), AIAA Journal, 2005-1405

[14] Heathcote, S., Martin, D., "Gursul, I., Flaxible flapping airfoil propulsion at zero freestream velocit", AIAA journal, No.42, 2004, pp.2196-2205.

[15] Dickonson, M. H., "Wing rotation and the aerodynamic basis of insect flight", Science, No. 284, 1999, pp. 1954-1960.